Direct bioelectrocatalysis by redox enzymes immobilized in electrostatically condensed oppositely charged polyelectrolyte electrode coatings

Journal:	*Analyst*
Manuscript ID	AN-ART-10-2019-002168.R1
Article Type:	Paper
Date Submitted by the Author:	04-Dec-2019

Complete List of Authors:	Lim, Koun; University of Utah, Department of Chemistry Sima, Monika; University of Utah Stewart, Russell J.; University of Utah Minteer, Shelley; University of Utah, Department of Chemistry

ARTICLE

Received 00th January 20xx,
Accepted 00th January 20xx

DOI: 10.1039/x0xx00000x

Direct bioelectrocatalysis by redox enzymes immobilized in electrostatically condensed oppositely charged polyelectrolyte electrode coatings

Koun Lim[a], Monika Sima[b], Russell J. Stewart[b], Shelley D. Minteer[a]

The Immobilization of enzymes on an electrode surface is critical in preserving enzyme activity and providing a sufficient electron transfer pathway for bioelectrocatalysis. Here, we present a novel single-step, cross-linker free immobilization for direct bioelectrocatalysis using an ionic strength induced phase inversion of oppositely charged polyelectrolytes. Cationic poly-guanidinyl-propyl-methacrylate (pGPMA, PG) and anionic inorganic polyphosphate, sodium hexametaphosphate (P6) were used to make electrostatically condensed phase (PGP6). A mixture of PGP6 and laccase (LAC) from *Tramates versicolor* or HRP (HRP) from *Armoracia rusticana* was deposited on the electrode surface and was submerged in DI water to form white porous electrode coatings. Each electrode showed a current generation corresponding respective substrates via direct bioelectrocatalysis.

Introduction

Oxidoreductases are a class of enzymes that have the ability to catalyze redox reactions in living organisms[1, 2]. Starting in the early 1960s, attempts were made to immobilize a variety of oxidoreductase onto the surface of an electrode, which sparked the research field of bioelectrocatalysis with applications to biosensors, biofuel cells, and bioelectronics[3-6]. Immobilization of enzymes to achieve bioelectrocatalysis must meet a crucial requirement - the immobilized oxidoreductase must establish a facile electron transfer path to and from the electrode[7, 8]. In such a case, the specific substrate undergoes oxidation or reduction catalyzed only by the immobilized oxidoreductase, and the electrons used in that redox reaction are monitored at the electrode surface. Mediated electron transfer (MET) and direct electron transfer (DET) are two-electron transfer paths established by the immobilized oxidoreductases. MET refers to an electron shuttle system using reversible redox-active molecules. These molecules undergo a rapid reduction and oxidation between the electrode surface and oxidoreductases to shuttle electrons between the enzyme and the electrode to complete the enzymatic reaction[9, 10]. On the contrary, DET refers to unassisted, distance-dependent tunneling of electrons between active sites of the oxidoreductase and the electrode surface[11, 12]. Both electron transfer paths are common in bioelectrocatalysis.

Generally, enzyme immobilization strategies involve physical adsorption, electrostatic adsorption, entrapment, and covalent attachment[13, 14]. A typical procedure involves covalently cross-linking the target protein to a polymer matrix for entrapment. The benefit of using a polymer matrix is its ability to facilitate both MET and DET via grafting different redox-active pendant or pyrene moieties on the backbone of the polymer[15-18]. However, the use of chemical cross-linkers sacrifices residual enzyme activity after immobilization due to denaturation resulting from covalent binding of nucleophilic sites of enzymes and activity loss from rigidity restricting enzyme function[19-21]. Also, depending on the choice of the cross-linkers, the curing time can be long enough to cause thermal destabilization of enzymes. One method to avoid cross-linkers for enzyme immobilization is layer-by-layer (LBL) enzyme absorption. Historically, LBL enzyme absorption by creating a multi-layer of enzyme and polyelectrolytes (PE) have shown to achieve bioelectrocatalysis at its most advantageous condition of mild working conditions in aqueous solution and its flexibility in obtaining different immobilization structures [22-27]. These PE layers could immobilize enzymes *via* physical entrapment or charge interaction. Water-soluble enzymes have a certain degree of surface charges in solution, and the oppositely charged PEs interact with the surface charges of enzymes and other charges of PEs in order to create an enzyme-PE layer. However, the LBL method is a multi-step procedure with a risk of thermal destabilization of enzymes. Thus, we present a convenient one-step method to immobilize redox enzymes on electrodes based on ionic strength induced

a. *Department of Chemistry, University of Utah, Salt Lake City, Utah, 84112, USA. E-mail: minteer@chem.utah.edu*
b. *Department of Biomedical Engineering University of Utah Salt Lake City, Utah, 84112, USA. E-mail: russell.stewart@utah.edu*
†Electronic Supplementary Information (ESI) available. See DOI: 10.1039/x0xx00000x

phase inversion of electrostatically condensed oppositely charged PEs.

Depending on the solution conditions, sets of oppositely charged water-soluble PEs can exist in several morphologies ranging from solutions, to colloidal suspensions of PE complexes, to concentrated phase-separated fluids (complex coacervates), to ionic solids[28, 29]. The morphology of a given set of condensed PEs is determined by solution conditions that affect the positive to negative charge ratio and the strength of electrostatic interactions, conditions that can include pH, dielectric constant, and ionic strength (I)[30]. The solution I is a convenient means to control the degree of counterion shielding between the polymeric charges, and thereby the morphology of the PEs. At monovalent ion concentrations above a critical I, the PEs are completely dissolved. At intermediate salt concentrations, the PEs associate dynamically and condense into a phase-separated liquid morphology, known as a complex coacervate. At low I, the PEs condense further into solid morphologies. The morphology can be transformed from the condensed fluid to the condensed solid morphology by changing the concentration of monovalent counterions in the environment[31].

The PEs used to form the electrode coating described here were cationic poly-guanidinyl-propyl-methacrylate (pGPMA)[32], and anionic inorganic polyphosphate, sodium hexametaphosphate (P6). The ionic strength induced phase inversion of a polyguanidinium and polyphosphate complex coacervate was previously reported[31]. At high NaCl concentrations, this PE system forms a phase-separated low viscosity adhesive fluid that can be applied to and spread as a thin layer on electrode surfaces, wet or dry. When introduced into a low I aqueous solution, the thin fluid coating undergoes rapid phase-inversion into a solid microporous coating. Including enzymes in the adhesive fluid creates a simple one-step method to surface-immobilize enzymes in dimensionally stable surface coatings. Because the system is entirely aqueous and requires no covalent crosslinking reactions, enzymes mixed into the fluid phase retain their structure and activity. We demonstrate DET from laccase and horseradish peroxidase immobilized in the PGP6 electrode coatings.

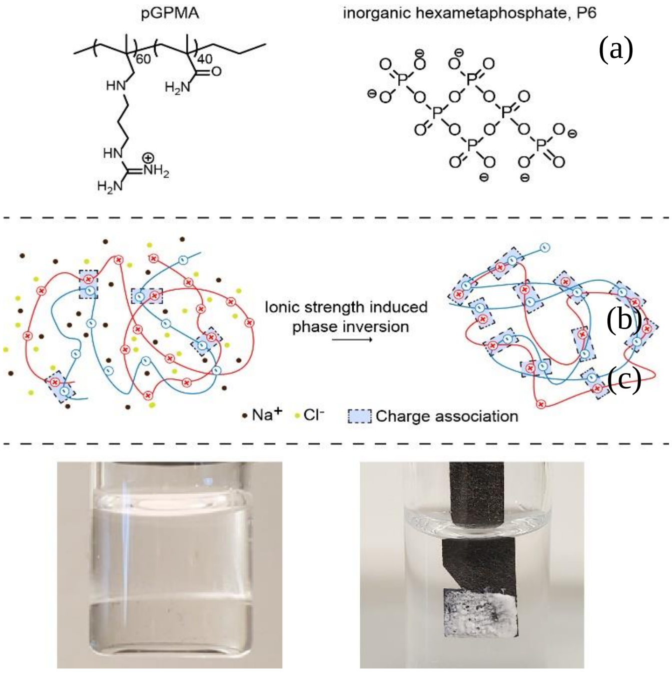

Figure 1. Ionic strength induced phase inversion of PGP6 complex coacervates into porous solid electrode coatings. PGP6 chemical structures (a) is shown with the appropriate mol ration of guanidinium side group. The illustrative scheme (b) shows the dynamic ionic interactions between PG (red line), P6 (blue line), and monovalent ions (solid dots) for the phase inversion of PGP6. The corresponding photos (c) of the different phases as a condensed liquid and white porous solid coating of PGP6

Results and discussion

Ionic strength induced phase inversion of PGP6 for enzyme immobilization

The PGP6 in 0.8 M NaCl was a condensed solution at the bottom of the scintillation vial, as shown in Figure 1 (left photo). In the condensed liquid form of PGP6, the charges of PEs are shielded by the surrounding salt ions, which shielded the associative ionic interactions of PEs. After the liquid PGP6 was deposited and spread onto a dry 0.25 cm^2 Avcarb electrode surface, the electrode was immersed in water. As the monovalent ions diffused out of the PGP6 layer, the oppositely charged PEs associated more strongly, resulting in a rapid phase inversion into a solid microporous coating, as shown in Figure 1 (right photo). Enzymes were immobilized in the coatings by adding up to 10% v/v of a solution of enzymes into the PGP6 liquid phase before electrode deposition. To ensure the enzyme entrapment, laccase was labeled with Fluorescein isothiocyanate. The labeled laccase was mixed with PGP6 at 10% v/v (PGP6-F-LAC). Under confocal fluorescence microscopy, the hydrated PGP6-F-LAC, as shown in Figure 2, showed a porous structure with ranging sizes and an even distribution of F-LAC throughout the solid phase of the electrode coating.

Bioelectrocatalysis of laccase from Trametes versicolor

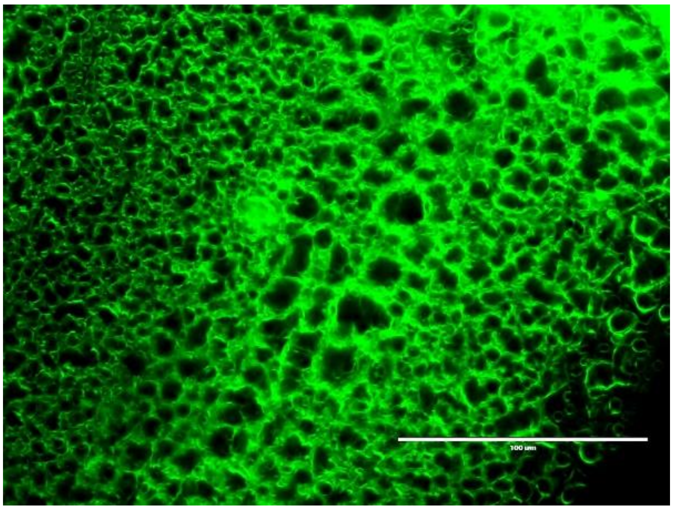

Figure 2. The confocal fluorescent microscope image of PGP6-F-LAC. Scale bar = 100 µM

The most crucial requirement of enzyme immobilization for bioelectrocatalysis is an establishment of electron transfer paths. Thus, laccase, an extensively researched enzyme known to facilitate DET, was loaded into the PGP6 coatings to confirm direct bioelectrocatalysis. At the active site of laccase, it has 3 copper cites critical to the catalytic function. A single copper entity is called T1 copper site (T1), and a cluster of three copper entities made up of one type 2 copper (T2), and a binuclear type 3 copper (T3) is called a trinuclear cluster (TNC). The T1 is responsible for gaining electrons from the oxidation of respective substrates or the electrode. Then, the collected electrons are transferred to the TNC, where a four-electron reduction of oxygen to water occurs[33, 34]. The onset potential of the oxygen reduction by laccase was near 0.6 V vs. SCE[16, 35, 36]. To confirm the reduction of O_2 to H_2O *via* DET of laccase, the CVs and SWVs of the PGP6-LAC electrodes were performed under aerobic and anaerobic environment.

Sweeping the potential window of CV from 0.8 V to 0.3 V vs. SCE, the catalytic currents recorded corresponded to the reduction of O_2 to H_2O by laccase with the approximated onset potential at 0.65 V vs. SCE as shown in Figure 3a. In order to confirm that the electrochemical response was *via* DET, SWV was performed. Sweeping in a forward direction, as shown in Figure 3b, a reduction peak of the T1 in the active site of laccase was observed at 0.61 V vs. SCE, confirming the onset potential observed for CV. Sweeping in the reverse direction, as shown in Figure 3c, the oxidation peak of the T1 was, once again, observed. This observation indicated the reversibility of the active redox center of laccase. On the other hand, the control electrode without laccase loading did not show a visible redox activity from the given potential range from the CVs and the SWVs. Therefore, the PGP6-LAC was deduced to reduce oxygen to water *via* DET. An optimization of deposition volume, dithiothreitol treatment to reverse the chloride inhibition of laccase and the enzyme loading into the PGP6 coatings were performed using CVs and shown in Figure S5, S6, and S7, respectively[37].

Bioelectrocatalysis of horseradish peroxidase from Armoracia rusticana

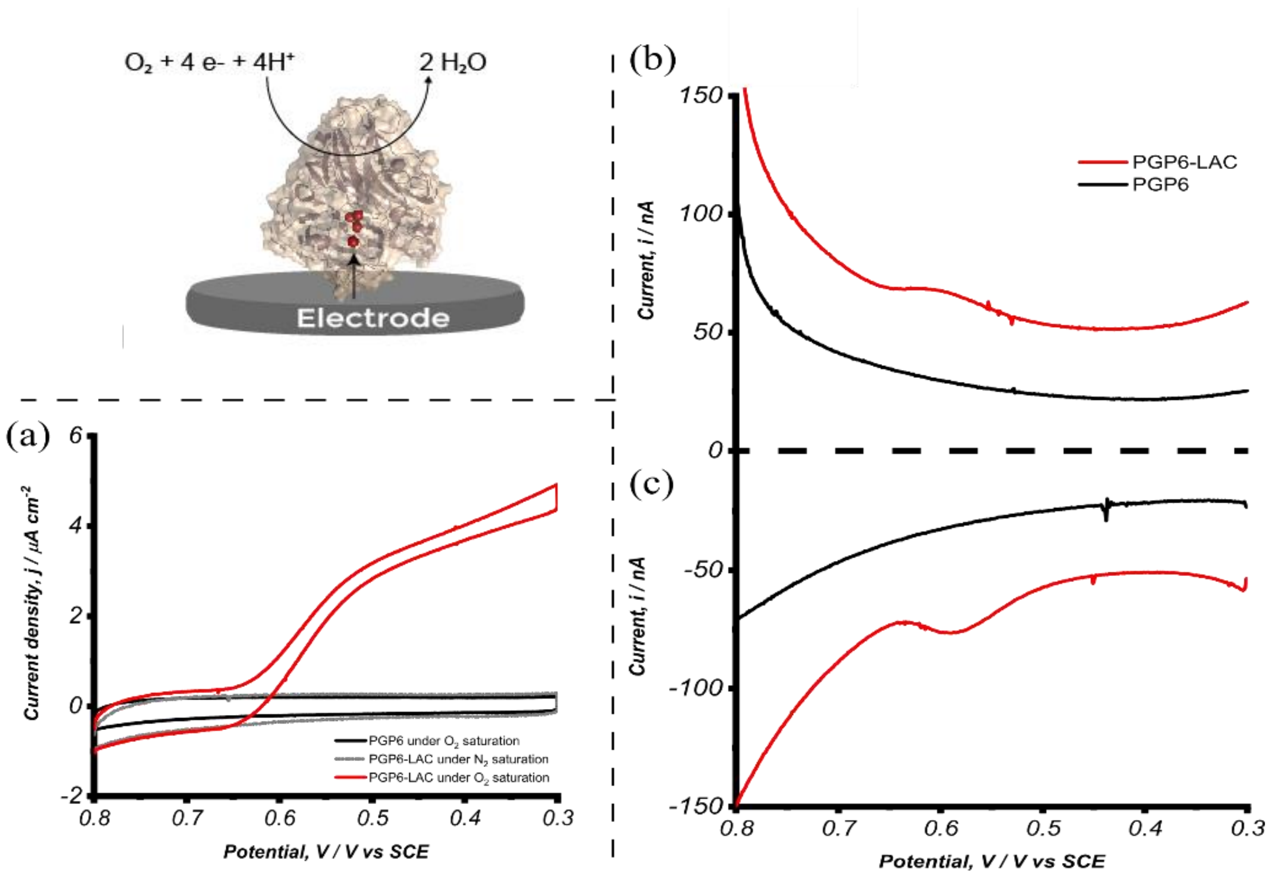

Figure 3. Representative electrochemical measurements of PGP6-LAC electrodes. All tests were performed in 100mM acetate buffer at pH 4.5. The cyclic voltammetry (a) was performed at a scan rate of 5 mV s^{-1}. The square wave voltammetry (b), (c) was performed using 1 mV increment, 1 mV amplitude and frequency at 1Hz. The control electrode was deposited using PGP6 and water and tested under O_2 saturation. The blank electrode, grey line, was deposited using active laccase and PGP6 and tested under N_2 saturation. The test electrode, red line, was deposited using active laccase and PGP6, tested under O_2 saturation.

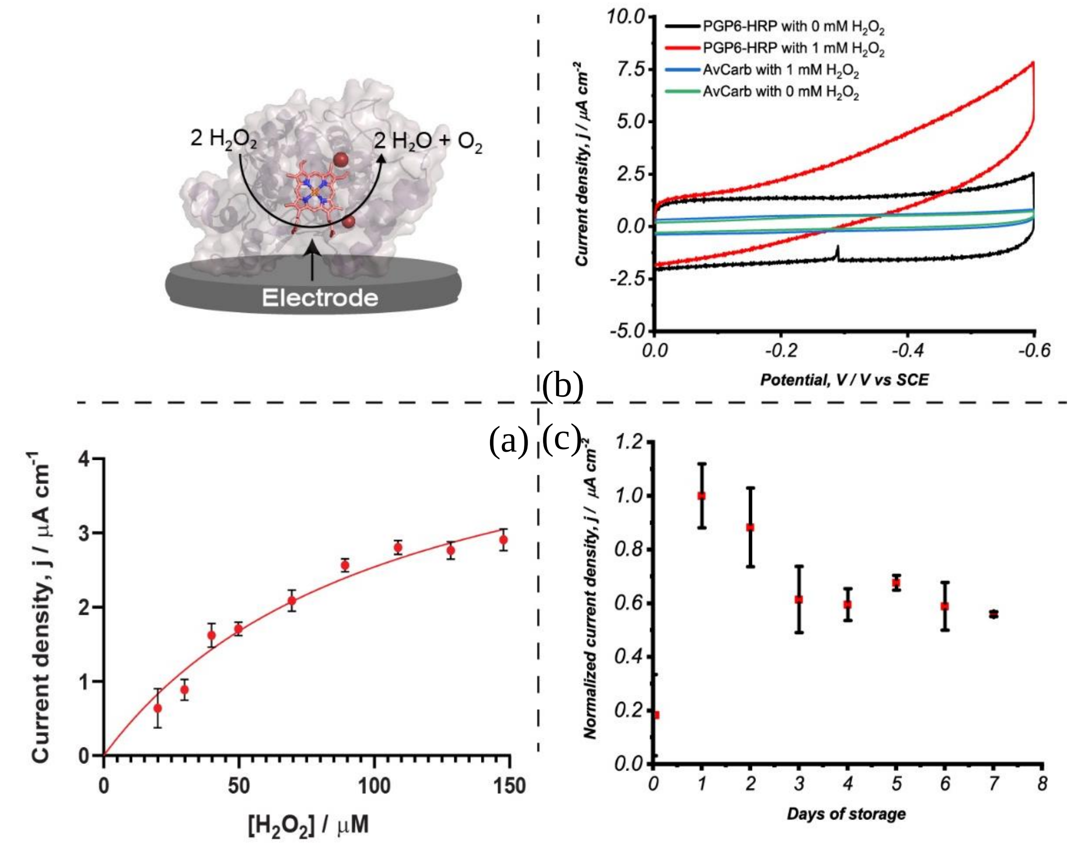

Figure 4. Representative electrochemical measurements of PGP6-HRP electrodes. All tests were performed in 100mM MOPS buffer at pH 7. The Michaelis–Menten enzyme kinetic (a) for PGP6-HRP was performed via amperometry held at -0.5 V vs SCE. The cyclic voltammetry (b) was performed at a scan rate of 5 mV s^{-1} using PGP6-HRP and a blank electrode, AvCarb. The 7-day stability test, reported as a normalized current density (c) was performed using amperometry held at -0.5 V vs SCE.

Confirming the DET of laccase immobilized in PGP6 coatings led to us investigating horseradish peroxidase (HRP), an enzyme known to facilitate the reduction of hydrogen peroxide *via* DET, to further show the flexibility of PGP6 as an enzyme immobilization support in the negative potential region.

Sweeping the potential window of CV from 0 V to -0.6 V vs. SCE, the catalytic currents recorded corresponding to the addition of H_2O_2 with the approximated onset potential at -0.1 V vs. SCE as shown in Figure 4b. Comparing to the previously published onset potential for DET of HRP around -0.3V vs. SCE[38-40], the observed onset potential of PGP6-HRP was shifted towards the positive region. A comparison of SWVs using a blank electrode, AvCarb, without any PGP6 and enzyme loading, a control electrode, PGP6, without enzyme loading and PGP6-HRP electrodes was constructed to investigate a shift in the onset potential and to confirm that the current response of H_2O_2 reduction was *via* DET of HRP.

Sweeping an extensive range of potentials from 0.3 V to -0.6 V vs. SCE, as shown in Figure 5, a defined reduction peak at -0.1 V vs. SCE was observed for all three electrodes, indicating the shifted onset potential observed for CVs was possibly due to an impurity from bare AvCarb electrodes. Also, as shown in Figure S8, the blank electrode slightly responded to the addition of 1M hydrogen peroxide with the onset potential around -0.1 V vs. SCE, and the overlay of the direct hydrogen peroxide reduction to the catalytic current observed by HRP is shown in Figure 4a. While the current contribution may be negligible, the effect of capacitive current with PGP6-HRP can show the onset potential of direct hydrogen peroxide more obvious. Thus, the positive shift of electrodes could be a result of both the impurity of AvCarb electrodes and the direct reduction of hydrogen peroxide.

Also, shown in Figure 5a, there was an observable peak around -0.4 V vs. SCE, matching with the literature value of the heme active site within HRP. Understanding the current contribution of direct hydrogen peroxide reduction was negligible, the catalytic current observed in Figure 4a was deduced to be DET of HRP responding to the addition of hydrogen peroxide.

The feasibility of PGP6-HRP as a working biosensor was assessed by the evaluation of the Michaels-Menten kinetics shown in Figure 4a and the 7-day stability test shownin figure 4c. The Michaelis–Menten kinetics (K_M) of the direct bioelectrocatalysis of PGP6-HRP was evaluated by non-linear regression and reported an apparent Michaelis–Menten constant (K_m^{app}) of 105.8 μM, with an associated maximum current density of 5.2 μA cm^{-2}. The K_m^{app} of PGP6-HRP was nearly 1 order of magnitude smaller than those reported K_m^{app} of other HRP biosensors using comparable polyelectrolyte LBL system such as quaternized poly(4-vinylpyridine)[41] (4.3 mM), quaternized poly(4-vinylpyridine) complexed of $(Os(bpy)_2Cl)^{+/2+}$ (3.4 mM)[42], nanocomposite of methylene blue multiwalled carbon nanotubes (3.56 mM)[43]. On the other hand, the linear detection range of PGP6 was 19 µM to 30 µM while the previously compared LBL system showed a linear range varying from 1 µM to 4 mM. Based on this comparison, PGP6 shows a promising H_2O_2 substrate affinity but suffers from the low range of the detection limit.

The durability of PGP6-HRP coating over time was evaluated by the 7-day stability test with the day when PGP6-HRP electrodes were made was considered as Day 0. The PGP6-HRP electrodes showed the highest current density of 3.6 µA cm^{-2} on day 1, and the initial decrease in the total current density was observed until the stabilization of the current density after day 3. It is deduced that from day 1 to day 3, the entrapped HRP within the PGP6 coatings gradually leached out until the equilibrium was achieved. After the equilibrium was achieved, the PGP6-HRP electrodes maintained its electrochemical activity, suggestive of stable entrapment. This result shows PGP6 a promising application as-needed enzyme immobilization method.

Experimental

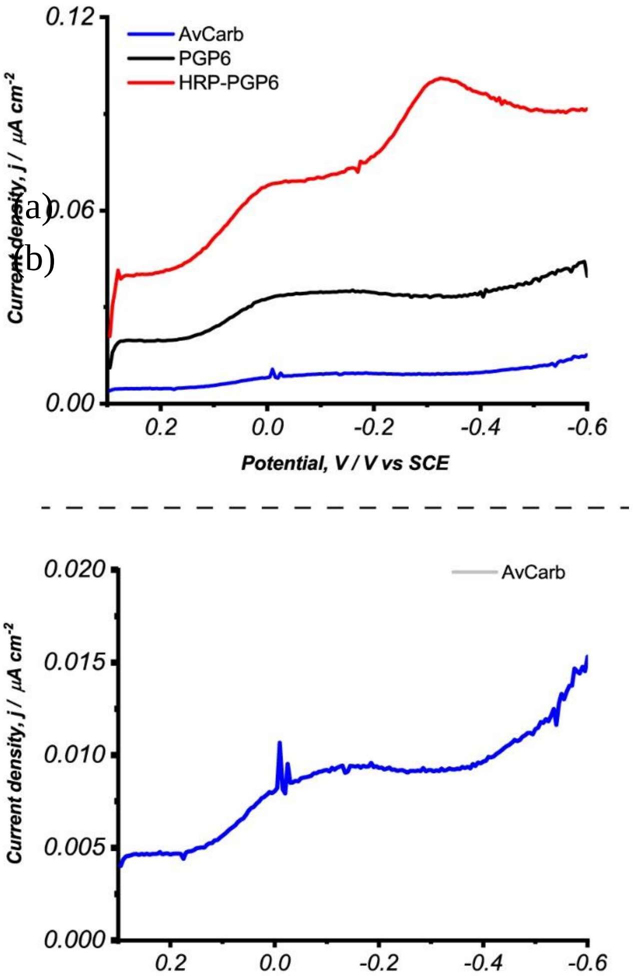

Figure 5. A comparison of representative square wave voltammograms (a) of PGP6-HPR, PGP6, and AvCarb electrodes. An enlarged SWV of AvCarb electrode (b) was separately shown. All SWVs were performed at 5 mV increment, 5 mV amplitude, and the frequency at 1 Hz on the second day of storing the PGP6-HRP electrodes.

Chemicals

Purified laccase (LAC) was purchased from Amano Enzyme Inc. Horseradish peroxidase (HRP) was purchased from Sigma Aldrich. Acetic acid (MFCD0003615), triethylamine (TEA, BP616-500), acetone (A18-20), methanol (A412-20), and ethyl ether anhydrous (EE, E138-20) were purchased from Fisher Chemical. Lithium bromide was purchased from MP Biomedicals. Ethylene glycol diglycidyl ether (EGDGE) and *N*-(3-Aminopropyl)methacrylamide hydrochloride (APMA•HCl) were purchased from Polysciences, Inc. N,N- Dimethylformamide (DMF, 22915) and methacrylamide (MA, L15013) were purchased from Alfa Aesar. 4-methoxyphenol (M0123) was purchased from Tokyo Chemical Industry Chemicals and *1H*-Pyrazole-1-Carboxamidine hydrochloride (PCA, 21678) was purchased from Chem-Impex International. Avcarb paper (MGL190) was purchased from Fuel Cell Store and was pre-cut into 0.25 cm^2 electrodes. Water used was filtered with Ultrapure Milli-Q system. All other chemicals used were purchased from Sigma Aldrich and used as received without further purification.

Synthesis of N-(3-methacrylamidopropyl)guanidinium chloride (GPMA)

GPMA was synthesized as previously described[32] with some modifications. Briefly, APMA•HCl (25g) and 4-Methoxyphenol (0.250g) were dissolved in 140mL DMF, Triethylamine (17g) was added to the reaction mixture and was under stirring for 10 minutes prior to the addition of *1H*-Pyrazole-1-carboxamidine monohydrochloride (20.51g), the flask was closed with a septum cap and the reaction mixture was kept under stirring for 17 hours. At the end of the reaction, the TEA•HCl salt was filtered off. For the extraction, the resulting oil was poured into ethyl ether under vigorous stirring until the oil is completely dispersed in the solvent. Then, the mixture was left to settle without stirring, and the solvent was decanted. The process was repeated using the following volumes of ethyl ether: 1) 4x the volume of the oil, 2) 3x the volume of the oil, and 3) 2x the volume of the oil. The GPMA monomer oil was analyzed by ^{1}H NMR and HPLC, as shown in Figure S1 and S2, respectively.

Synthesis of the synthetic polycationic polymer P-(GPMA-co-MA), (PG)

The synthesis of P-(GPMA-co-MA) was synthesized as previously described[32], using conventional free radical polymerization. The copolymer composition has 60 mol% GPMA and 40 mol% methacrylamide. The V-501 initiator comprises 3% (weight/volume) of the reaction mixture, total monomer concentration is 1 M in 60% water/ 40% methanol . The required amount of GPMA was dissolved in de-ionized H_2O and transferred into a round bottom flask, where dry methacrylamide, V-501, and methanol were added to the mixture. The reaction mixture was degassed with nitrogen gas for 60 min and was polymerized under N_2 at 70° C for 3 hours. The reaction was quenched by exposure to oxygen for 15 minutes. The cooled reaction mixture was precipitated into acetone under constant stirring. The precipitated polymer was filtered off and dried under vacuum. The polymer was further purified using a Millipore ultrafiltration system with Pellicon 2 Mini Cassette (Biomax 5 kDa), first using 10x volume exchange of 150mM NaCl pH 3 (1mM HCl) and 20x volume exchange using de-ionized water. The purified polymer was lyophilized. The polymer was characterized using GPC and the ^{1}H NMR, as shown in Figure S3 and S4. The chemical structure of the final product, P-(GPMA-co-MA), is shown in Figure 1A.

Complex coacervation of (PGP6) from p(GPMA-co-MA) (PG) and sodium hexametaphosphate (P6)

This preparation protocol describes a 10 ml batch yields 800 uL of the coacervate. A 200 mg ml^{-1} stock solution of sodium hexametaphosphate and a 100 mg ml^{-1} stock solution of PG were prepared using de-ionized water. The pH of both solutions was adjusted to 7.2~7.4 using 6M NaOH and 1M HCl. 1.2 ml of 5M NaCl, 1.915 ml of de-ionized water and 1.885 ml of P6 were mixed and vortexed. Into the mixture, 5 ml of PG was added to achieve a charge ratio of 2:1 (P6: PG) and a final concentration of 800mM NaCl. The formed PGP6 was left at 20-22°C to equilibrate without any mixing/vortexing for at least 12 hours. The sample was centrifuged for 5 minutes at 2000RPM at room temperature, the supernatant was removed, and these steps were repeated once more. In order to change the coacervate to the desired final salt concentration, the required amount of 5M NaCl was added to the sample and was agitated gently for a few hours.

Electrode fabrication

A stock solution of 50 mg ml^{-1} LAC and HRP were prepared using purified water. A total of 20 µL PGP6 – enzyme mixture was made by mixing 18 µL of PGP6 and 2 µL of each enzyme solution. On to the pre-cut 0.25 cm^2 AvCarb electrode surface, 1.5 µL of this mixture was deposited. These electrodes were immersed in water for at least 30 minutes to harden the coating. In the case of PGP6-laccase (PGP6-LAC) electrodes, the electrodes were immersed in a fresh solution of 1 mM dithiothreitol (DTT) prior to any electrochemical testings. In the case of PGP6 – horseradish peroxidase (PGP6-HRP), all the electrode fabrication was done under anaerobic conditions.

Laccase bioelectrocatalysis

Cyclic voltammetry(CV) and square wave voltammetry (SWV) of PGP6-LAC electrodes were performed at room temperature using 10 mL of 100 mM acetate buffer of pH 4.5 from 0.8 V vs. SCE to 0.3 V vs. SCE. The CV was performed at 5 mV s^{-1}, and the SWV was performed using 1 mV increment, 1 mV amplitude, and the frequency at 1 Hz. The buffer was purged with O_2 for 10 minutes before the electrochemical testing and continued the purge unless stated otherwise. For all electrochemical testings of PGP6-LAC, CH instrument 660 E potentiostat (CH Instruments, Austin, TX) with a 3-electrode system using a saturated calomel electrode (SCE) as a reference, Pt mesh electrodes as a counter electrode and PGP6-LAC as working electrodes.

Horseradish peroxidase bioelectrocatalysis

The CV and SWV of PGP6-HRP electrodes were performed under anaerobic conditions using 10 mL of 100 mM MOPS buffer at pH 7.0 from 0.1 V vs. SCE to -0.7 V vs. SCE. The CV was performed at 5 mV s^{-1}, and the SWV was performed using 5 mV increment, 5 mV amplitude, and the frequency at 1 Hz using the PGP6-HRP electrodes on the second day of storage. The amperometric responses of PGP6-HRP to H_2O_2 injections were performed at -0.5 V vs. SCE in 5 ml of 100 mM MOPS buffer while stirred. In the case of storage stability, a total of 21 PGP6-HRP electrodes were made following the electrode fabrication protocol under anaerobic conditions. To ensure triplication of the stability test, these PGP6-HRP electrodes were stored in groups of 3 in a scintillation vial with 16 ml of water. These containers were sealed with a cap and were stored at 4°C until the day of testings. The amperometric responses were performed at -0.5 V vs. SCE in 5 ml of 100 mM MOPS buffer while stirred. The background current was measured for 100 seconds, and then, the current response to the addition of 100 µL of 10 mM H_2O_2 was monitored for 600 seconds. For all electrochemical testings of PGP6-LAC, CH instrument 1230 A potentiostat (CH Instruments, Austin, TX) with a 3-electrode system using a saturated calomel electrode (SCE) as a reference, Pt mesh electrodes as a counter electrode and PGP6-HRP as working electrodes. The Michaelis–Menten value was calculated using GraphPad prism 8.

Fluorescent confocal microscope

Laccase (LAC) was labeled with fluorescein isothiocyanate (FITC) via the following procedure. A stock solution of 2 mg ml^{-1} laccase was made using DI water, and a stock solution of 1 mg ml^{-1} FITC was made using DMSO. A mixture containing 1 mL of LAC stock solution and 0.1 ml of FITC stock solution was stirred at 4°C for 3 hours and then stirred overnight at room temperature. The mixture was purified on PD-10 column and freeze dried. A solution of 0.28 mg ml^{-1} fluorescein-labelled LAC (F-LAC) and 28 mg ml^{-1} unlabeled laccase were prepared. A mixture of these LAC solutions was made by mixing 1 µL of F-LAC and 2 µL of unlabelled laccase solution. For depositing a thin film for the microscopy, a solution was made by mixing 27 µL of PGP6 and 3 µL of the F-LAC mixture solution. A thin layer was made on a glass coverslip by physically spreading 3 µL of the PGP6-F-LAC. The coating was solidified by dipping the glass coverslip in water. These thin films were stored in water for 24 hours in the dark to avoid photobleaching. All of the fluorescent images were taken using Nikon A1 HD25 confocal microscope at 500 nm.

Conclusion

This paper investigated a one-step enzyme immobilization using a complex coacervate, PGP6, *via* ionic-strength induced phase inversion. Its ability to facilitate DET with an enhanced sensitivity was confirmed using LAC and HRP at both positive and negative potentials. These coated electrodes were ready for electrochemical testings within an hour after preparation, and its maximum current in response to the corresponding substrate was observed within 24 hours, indicative of its potential use as rapid enzyme immobilization matrix. Utilizing its convenience, PGP6 can be applied in flow-through cells for a wastewater management system and urgent enzymatic biosensors using a variety of enzymes. Further advancing the stability of coatings for long-term electrochemical testings and lowering the limit of detection will be researched for improving the applicability of PGP6 as enzyme immobilization matrix. Moreover, an additional benefit of PGP6 is its flexibility on modification with other redox moieties to facilitate MET. A majority of oxidoreductases have their cofactor buried inside of polypeptide shell which makes DET unfavorable. Hence, MET using small redox molecules has been established for establishing bioelectrocatalysis. Therefore, modification of PGP6 will be an influential achievement in broadening enzyme choices for biofuel cell and biosensor applications.

Conflicts of interest

There are no conflicts to declare.

Acknowledgments

Imaging was performed at the Fluorescence Microscopy Core Facility, a part of the Health Sciences Cores at the University of Utah. Microscopy equipment was obtained using an NCRR Shared Equipment Grant # 1S10RR024761-01. RJS acknowledges funding from the Office of Naval Research (Award # N000141612538)

Notes and references

1. S. W. May and S. R. Padgette, *Nature Biotechnology*, 1983, **1**, 677-686.
2. L. Sellés Vidal, C. L. Kelly, P. M. Mordaka and J. T. Heap, *Biochim Biophys Acta Proteins Proteom*, 2018, **1866**, 327-347.
3. N. J. Ronkainen, H. B. Halsall and W. R. Heineman, *Chemical Society Reviews*, 2010, **39**, 1747-1763.
4. H. A. Abdulbari and E. A. M. Basheer, *ChemBioEng Reviews*, 2017, **4**, 92-105.
5. D. Grieshaber, R. MacKenzie, J. Vörös and E. Reimhult, *Sensors*, 2008, **8**.
6. M. Rasmussen, S. Abdellaoui and S. D. Minteer, *Biosensors and Bioelectronics*, 2016, **76**, 91-102.
7. R. D. Milton, T. Wang, K. L. Knoche and S. D. Minteer, *Langmuir*, 2016, **32**, 2291-2301.
8. K. Habermüller, M. Mosbach and W. Schuhmann, *Fresenius' Journal of Analytical Chemistry*, 2000, **366**, 560-568.
9. P. Kavanagh and D. Leech, *Physical Chemistry Chemical Physics*, 2013, **15**, 4859.
10. M. E. G. Lyons, *Electroanalysis*, 2015, **27**, 992-1009.
11. R. D. Milton and S. D. Minteer, *J R Soc Interface*, 2017, **14**, 20170253.
12. R. S. Freire, C. A. Pessoa, L. D. Mello and L. T. Kubota, *Journal of the Brazilian Chemical Society*, 2003, **14**, 230-243.
13. N. R. Mohamad, N. H. C. Marzuki, N. A. Buang, F. Huyop and R. A. Wahab, *Biotechnology, biotechnological equipment*, 2015, **29**, 205-220.
14. S. Datta, L. R. Christena and Y. R. S. Rajaram, *3 Biotech*, 2013, **3**, 1-9.
15. R. D. Milton, D. P. Hickey, S. Abdellaoui, K. Lim, F. Wu, B. Tan and S. D. Minteer, *Chemical Science*, 2015, **6**, 4867-4875.
16. D. P. Hickey, K. Lim, R. Cai, A. R. Patterson, M. Yuan, S. Sahin, S. Abdellaoui and S. D. Minteer, *Chemical Science*, 2018, **9**, 5172-5177.
17. R. D. Milton, K. Lim, D. P. Hickey and S. D. Minteer, *Bioelectrochemistry*, 2015, **106**, 56-63.
18. S. Abdellaoui, R. D. Milton, T. Quah and S. D. Minteer, *Chemical Communications*, 2016, **52**, 1147-1150.
19. S. Avrameas and T. Ternynck, *Immunochemistry*, 1969, **6**, 53-66.
20. I. Migneault, C. Dartiguenave, M. J. Bertrand and K. C. Waldron, *BioTechniques*, 2004, **37**, 790-802.
21. X. Lu, Y. Xu, C. Zheng, G. Zhang and Z. Su, *Journal of Chemical Technology & Biotechnology*, 2006, **81**, 767-775.
22. O. S. Sakr and G. Borchard, *Biomacromolecules*, 2013, **14**, 2117-2135.
23. K. Ariga, Q. Ji and J. P. Hill, in *Modern Techniques for Nano- and Microreactors/-reactions*, ed. F. Caruso, Springer Berlin Heidelberg, Berlin, Heidelberg, 2010, pp. 51-87.
24. F. N. Crespilho, M. Emilia Ghica, M. Florescu, F. C. Nart, O. N. Oliveira and C. M. A. Brett, *Electrochemistry Communications*, 2006, **8**, 1665-1670.
25. J.-J. Feng, J.-J. Xu and H.-Y. Chen, *Biosensors and Bioelectronics*, 2007, **22**, 1618-1624.
26. M. Ferreira, P. A. Fiorito, O. N. Oliveira and S. I. Córdoba de Torresi, *Biosensors and Bioelectronics*, 2004, **19**, 1611-1615.
27. D. Cao and N. Hu, *Biophysical Chemistry*, 2006, **121**, 209-217.
28. H. Shao, K. N. Bachus and R. J. Stewart, *Macromolecular Bioscience*, 2009, **9**, 464-471.
29. Q. Wang and J. B. Schlenoff, *Macromolecules*, 2014, **47**, 3108-3116.
30. E. Spruijt, M. A. Cohen Stuart and J. van der Gucht, *Macromolecules*, 2013, **46**, 1633-1641.
31. J. P. Jones, M. Sima, R. G. O'Hara and R. J. Stewart, *Advanced Healthcare Materials*, 2016, **5**, 795-801.
32. L. J. Prather, G. M. Weerasekare, M. Sima, C. Quinn and R. J. Stewart, *Polymers*, 2019, **11**, 649.
33. S. M. Jones and E. I. Solomon, *Cellular and Molecular Life Sciences*, 2015, **72**, 869-883.
34. H. Komori, R. Sugiyama, K. Kataoka, K. Miyazaki, Y. Higuchi and T. Sakurai, *Acta Crystallographica Section D Biological Crystallography*, 2014, **70**, 772-779.
35. M. T. Meredith, M. Minson, D. Hickey, K. Artyushkova, D. T. Glatzhofer and S. D. Minteer, *ACS Catalysis*, 2011, **1**, 1683-1690.
36. R. D. Milton, F. Giroud, A. E. Thumser, S. D. Minteer and R. C. T. Slade, *Physical Chemistry Chemical Physics*, 2013, **15**, 19371-19379.

37. C. H. Kjaergaard, F. Durand, F. Tasca, M. F. Qayyum, B. Kauffmann, S. Gounel, E. Suraniti, K. O. Hodgson, B. Hedman, N. Mano and E. I. Solomon, *Journal of the American Chemical Society*, 2012, **134**, 5548-5551.
38. T. Ferri, A. Poscia and R. Santucci, *Bioelectrochemistry and Bioenergetics*, 1998, **44**, 177-181.
39. R. Villalonga, P. Díez, P. Yáñez-Sedeño and J. M. Pingarrón, *Electrochimica Acta*, 2011, **56**, 4672-4677.
40. Y. Wang, X. Ma, Y. Wen, Y. Xing, Z. Zhang and H. Yang, *Biosensors and Bioelectronics*, 2010, **25**, 2442-2446.
41. C. Sun, W. Li, Y. Sun, X. Zhang and J. Shen, *Electrochimica Acta*, 1999, **44**, 3401-3407.
42. W. Li, Z. Wang, C. Sun, M. Xian and M. Zhao, *Analytica Chimica Acta*, 2000, **418**, 225-232.
43. Y. Zhang, L. Liu, F. Xi, T. Wu and X. Lin, *Electroanalysis*, 2010, **22**, 277-285.

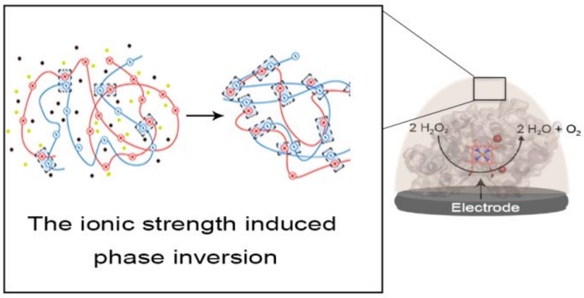

The ionic induced phase inversion of two oppositely charged electrolytes for enzyme immobilization and its application in bioelectrocatalysis